Focal Mechs: Distributions on Circles and Spheres

Jonathan M. Lees
University of North Carolina, Chapel Hill
Department of Geological Sciences
CB #3315, Mitchell Hall
Chapel Hill, NC 27599-3315
email: jonathan.lees@unc.edu
ph: (919) 962-1562

July 13, 2012

0.1 Directional Data: Circles

0.1.1 Statistics using circular or directional data

Since data in the earth sciences often involve spatially distributed information on the directionality of a particular property it is important for researchers in the geological sciences to have a firm grasp on the differences these data have with other scalar data. Advanced treatments of circular statistics can be found in [Fisher, 1993] and [Mardia, 1972].

Directions in the earth sciences arise in analysis of spatially oriented observations such as fault strikes, striations, mineral deformation or other data concerned with bearing. It is common for the uninitiated to make the mistake that angles can be treated like other Cartesian parameters. Angles are commonly recorded as data points in units of degrees, although these are not very useful for typical calculation. As a first step angles should transformed into radians using the conversion factor $\pi/180$ radians/degree. Once angles have been converted, they can be transformed to Cartesian coordinates using

$$\begin{aligned} x &= A\cos(\alpha) \\ y &= A\sin(\alpha) \end{aligned} \tag{0.1}$$

where the angle α increases from the x (bottom) axis counter-clockwise and A is the radius of the circle, here set to one. In many geological situations, however, angles are measured from the North clockwise. In that case, given data in degrees, we must reverse the direction and rotate by 90°.

$$\begin{aligned} x &= A\cos(90 - \alpha^\circ) \\ y &= A\sin(90 - \alpha^\circ) \end{aligned} \tag{0.2}$$

Again, angles presented in degrees and must be converted to radians prior to using trigonometric functions in R.

For example, if we have a set of angles a, provided as an example in Mardia(1972, p.22),

```
A = 1
##  a=c(41.9,31.7,48.2,42.4,32.8,36.0,28.6,33.2,34.3,32.5)
###   data from Mardia(1972) p 22
a = c(43,45,52,61,75,88,88,279,357)
x = A*cos((a)*pi/180)
y = A*sin((a)*pi/180)
n = length(a)
Mx = mean(x)
My = mean(y)
Mdir = (atan2(My, Mx))*180/pi
Rbar = sqrt(Mx^2+ My^2)
```

```
##  draw a circle
i=pi*(0:360)/180
cx =  A*cos(i);
cy =  A*sin(i);
```

which can be plotted with the code:

```
plot(cx, cy, type='n', asp=1, ann=FALSE, axes=FALSE)
lines(cx,cy)
points(x,y)
segments(0,0, x,y, col=grey(.7))
arrows(0,0, Rbar*cos(Mdir*pi/180  ) , Rbar*sin(Mdir*pi/180  ), col=grey(0))
```

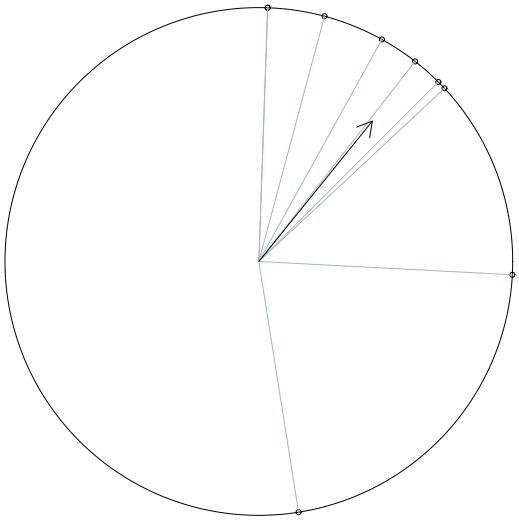

Figure 1: Circular plot of directions for FINLAND data set

For directional data a summary direction can be extracted by adding the x and y coordinates because they are Cartesian. If the directions are uniformly scattered, the resultant direction will be small. On the other hand if the directions cluster in a dominant orientation, the summed vectors will add constructively and the resultant will be large. As an example we use the data for a set of glacial striation directions from Finland (Davis, 2003, p.317). The average direction will be oriented towards the mean x and y values.

```
a=c(23,27,53,58,64,83,85,88,93,99,100,105,113,113,114,117,121,123,125,
126,126,126,127,127,128,128,129,132,132,132,134,135,137,144,145,145,146,153,155,155,
```

```
155,157,163,165,171,172,179,181,186,190,212)
x = A*cos((90-a)*pi/180)
y = A*sin((90-a)*pi/180)
Mx = mean(x)
My = mean(y)
Mdir = (pi/2-atan2(My, Mx))*180/pi
```

The mean direction of this data is thus α =129°. This can be added simply to the plot of the original data,

```
plot(cx, cy, type='n', asp=1, ann=FALSE, axes=FALSE)
lines(cx,cy)
points(x,y)
segments(0,0, x,y, col=grey(.8))
arrows(0, 0, Mx, My, lwd=2)
```

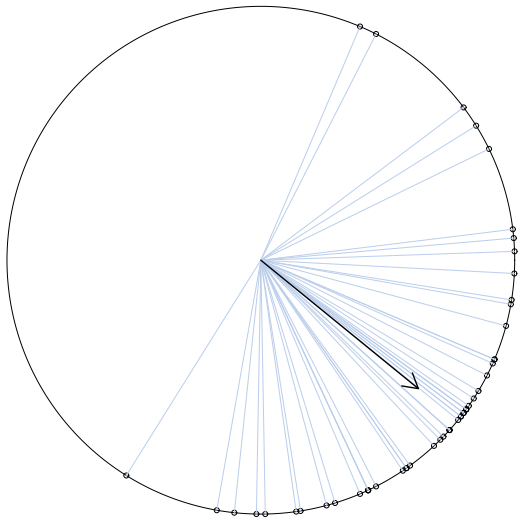

Figure 2: FINLAND data set with mean direction shown

The mean resultant length is often denoted $\bar{R}$ and is used in a variety of quantitative measures of the circular data set. for example, the circular variance is estimated by

$$S = 1 - \frac{R}{n} = 1 - \bar{R} \tag{0.3}$$

which in our case is,

```
R = sqrt(sum(x)^2+sum(y)^2)
Rbar = sqrt(Mx^2+ My^2)
S = 1 - Rbar
```

To perform hypothesis testing with circular data we use the von Mises distribution, or the circular normal distribution. This distribution is characterized by two parameters, κ and μ and is given by,

$$f(x \mid \mu, \kappa) = \frac{e^{\kappa cos(x-\mu)}}{2\pi I_0(\kappa)} \tag{0.4}$$

To illustrate this distribution with different levels of compaction κ we can generate distributions using R,

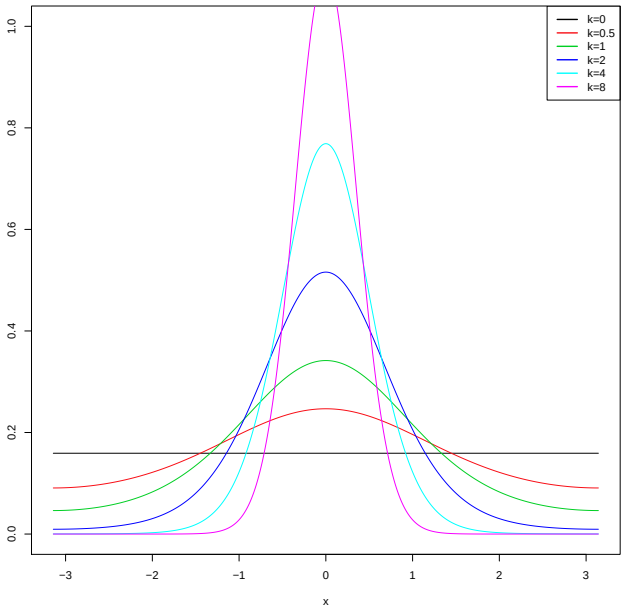

Figure 3: Probability Density Function for von Mises Distribution

The CRAN distribution site has a package called CircStats that has many of the functions used in analyzing circular data. Given a calculated $\bar{R}$ value one can get an estimate of the κ by loading the CircStats package and calling the est.kappa function.

```
library(CircStats)
kappa = est.kappa(a*pi/180)
mu = Mdir*pi/180
```

If the data were extracted from a uniform distribution we would expect the value of $\bar{R}$ to be small. A test due to Lord Rayleigh can be accomplished be comparing $\bar{R}$ to critical values for different P-values. A table of P-values can be found in Davis (Table A10) or Mardia (Appendix 2.5). Here we provide an approximation using a method devised by Wilkie(1983). The table data are recreated using R:

```
pees = c(0.1, 0.05, 0.025, 0.01)
n = c(4:25, 30, 35, 40, 45, 50)
On = 1/n
TAB = matrix(ncol=length(pees)+1, nrow=length(n))
TAB[,1] = n
for(i in 1:length(pees))
{
P = pees[i]
K = -log(P) - ( (2*log(P) + (log(P)^2) )/(4*n))
TAB[,i+1] = sqrt(K*On)
}
colnames(TAB)<-c("n",pees)
print(TAB)
```

```
      n       0.1      0.05     0.025      0.01
 [1,]  4 0.7515051 0.8380480 0.9082263 0.9817512
 [2,]  5 0.6734610 0.7545310 0.8218730 0.8950204
 [3,]  6 0.6155695 0.6917903 0.7560085 0.8271724
 [4,]  7 0.5704262 0.6424505 0.7037021 0.7724448
 [5,]  8 0.5339490 0.6023408 0.6608886 0.7271740
 [6,]  9 0.5036789 0.5689047 0.6250175 0.6889536
 [7,] 10 0.4780342 0.5404774 0.5944012 0.6561432
 [8,] 11 0.4559456 0.5159227 0.5678738 0.6275859
 [9,] 12 0.4366606 0.4944347 0.5446013 0.6024414
[10,] 13 0.4196323 0.4754243 0.5239693 0.5800831
[11,] 14 0.4044523 0.4584497 0.5055145 0.5600340
[12,] 15 0.3908088 0.4431716 0.4888793 0.5419235
[13,] 16 0.3784589 0.4293253 0.4737836 0.5254589
[14,] 17 0.3672104 0.4167003 0.4600039 0.5104058
[15,] 18 0.3569087 0.4051270 0.4473596 0.4965739
[16,] 19 0.3474280 0.3944672 0.4357030 0.4838068
[17,] 20 0.3386647 0.3846066 0.4249120 0.4719748
[18,] 21 0.3305328 0.3754503 0.4148845 0.4609693
[19,] 22 0.3229599 0.3669181 0.4055346 0.4506983
[20,] 23 0.3158847 0.3589422 0.3967894 0.4410839
[21,] 24 0.3092550 0.3514648 0.3885863 0.4320590
[22,] 25 0.3030259 0.3444359 0.3808716 0.4235657
[23,] 30 0.2766935 0.3146890 0.3481840 0.3875217
```

```
[24,] 35 0.2562147 0.2915194 0.3226842 0.3593437
[25,] 40 0.2396993 0.2728135 0.3020737 0.3365333
[26,] 45 0.2260145 0.2573005 0.2849666 0.3175783
[27,] 50 0.2144342 0.2441646 0.2704710 0.3015024
```

Once a significance level has been chosen, it can be compared to values in the table to determine the critical points for rejection. As shown in Davis, since $\bar{R}$ =0.8 is greater than the critical value from the table $\bar{R}_{50\,5\%}$ =0.244. Thus at 5% significance we reject the null hypothesis that the concentration parameter is zero and conclude that the data are not uniformly distributed.

0.1.2 Rose Diagrams

Rose diagrams are often used to represent graphically circular distributions of data in a way that is analogous to histograms. Serious problems can arise resulting in misleading readers if rose diagrams are done improperly. If the petals of a rose diagram are plotted with radii proportional to the *number* of samples in the bin, as opposed to the *area* of the petal plotted proportional to the number or percentage of the elements between two angles, the rose diagram will appear biased, or weighted improperly. To illustrate this we use a set of data from Davis called FINLAND.txt using the program rose.R supplied in the appendix.

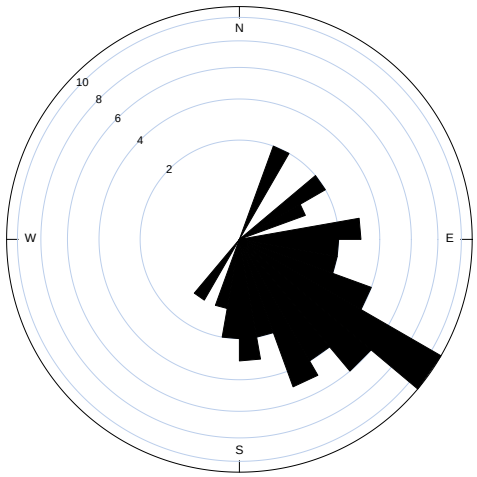

Figure 4: Simple Rose Diagram

Note that the scale is not linear. In the example and code provided here it is worthwhile noting that the rose diagram can be scaled and plotted anywhere on an existing plot made in R. For

example, if a map is plotted and circular rose diagrams are used to illustrate the spatial variation of orientations it is easy to create a complex plot of both map and roses together.

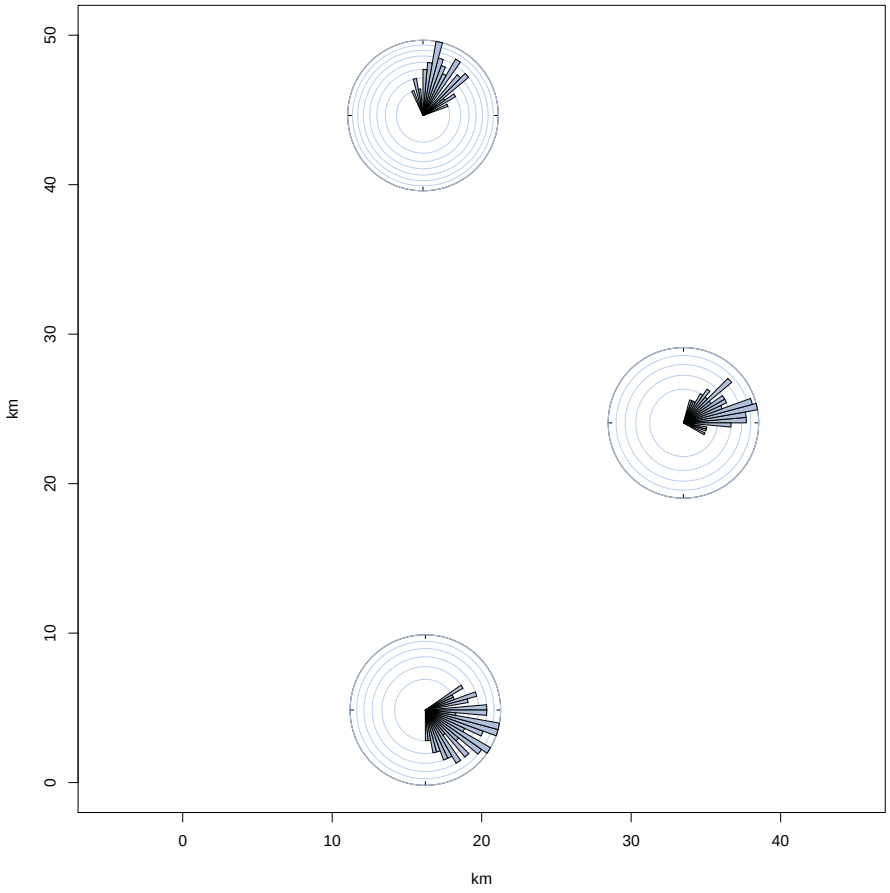

Figure 5: Geographic distribution of Rose diagrams

Here one can easily see the spatial variation of directional data across a field site. For each location a statistical test can be performed and confidence can be used to modify the roses by color or other method.

0.2 Data distributed on Spheres

Analysis of data on the sphere is critical to geological sciences for an obvious reason: the Earth can be approximated simply as a sphere to first order. Beyond this important motivation it spheres are used in geological sciences to represent the distribution of three-dimensional orientations and directions, the distribution of planar surfaces and, of course, as simplification of tensors (focal mechanisms).

This chapter includes analysis of upper and lower hemispheric projections of fault information, focal mechanisms, stress distributions and associated statistical tests. Examples from paleomagnetic data will be presented and rotations on the sphere will be discussed. This chapter ties in well with the section on Matrices. An excellent advanced book on this topic is [N. I. Fisher and Emgleton, 1987] and [Mardia, 1972].

0.3 Spherical Coordinate Systems

Geometry on the sphere is critical for Earth Science data analysis for obvious reasons, namely that the Earth is approximated to first order by a sphere. Locations on the planet are referenced via latitude (Lat) and longitude (Lon), and calculations related to positioning or distribution of properties on the globe are essential. Furthermore, many applications involving spherical distributions are common in structural geology and geophysics, where faults are represented as poles on and earthquake ruptures are modeled as double couple focal mechanisms using spherical relations between fault and auxiliary planes.

We first establish the relationship between Cartesian coordinate system (x, y, z) and spherical coordinate system (r, ϕ, θ). For many applications the mathematical definition stems from taking the x-axis on the page to the right, the y-axis is up, and the z-axis is out of the page. In that case r is the radius of the vector, ϕ is the angle from the zenith along the z-axis, and θ is the angle of the projection of the vector in the x-y plane with the x axis. The relationship between the Cartesian and the spherical coordinates is expressed as a transformation,

$$\begin{aligned} x &= r\cos(\theta)\sin(\phi) \\ y &= r\sin(\theta)\sin(\phi) \\ z &= r\cos(\phi) \end{aligned} \tag{0.5}$$

where the inverse relationships are,

$$\begin{aligned} r &= \sqrt{x^2 + y^2 + z^2} \\ \phi &= \cos^{-1}(z/r) \\ \theta &= \tan^{-1}(y/x) \end{aligned} \tag{0.6}$$

These are illustrated in the following diagram where the angles and the Cartesian axes are laid out. As noted earlier, it is conventional in geographical applications to use North facing up on the page. In that case the θ should be adjusted to represent increasing angle clockwise, or $\theta\prime = 90 - \theta$ when θ is in degrees. Also, the angle ϕ is co-latitude and if latitude is given it must be converted similarly, $\phi\prime = 90 - \phi$.

Once these relations are established and coded properly, converting coordinate systems in R is easy. Given a set of LAT-LON pairs, one converts to Cartesian coordinates, performs a calculation and converts back for further analysis. we saw this earlier in chapter 4 when we found the distance between Chicago and Paris using the cross product of two Cartesian vectors.

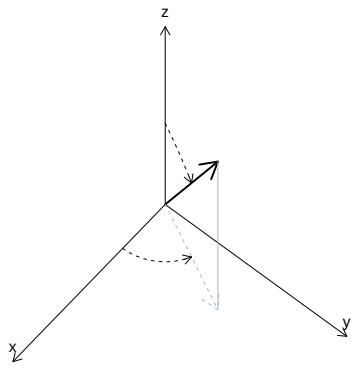

Figure 6: Coordinate system for geographic vectors and angles

0.4 Fisher Statistics

Data distributed on a sphere is quite common in Earth science. Problems that deal with fault distributions, focal mechanisms, and paleomagnetic poles are just a few examples. It is useful for a

researcher in geology to have at hand a set of tools ready for attacking such problem with ease and flexibility. While canned programs exist that allow users to dump in data sets, plot see summary statistics it is much more beneficial to be able to access data sets in minute detail while also having higher level graphical and analytical tools. The R platform is excellent for achieving this goal. As an example consider a set of paleomagentic poles observed from laboratory measurements of rocks collected across a large continental region. The research needs to know what the mean orientation of the magnetic poles are to see if the continent has rotated and move large distances in the north south direction.

From a set of N measurements the researcher has pairs of inclination and declination estimated in the lab. The first step is to plot these on a stereo net, either equal area (Schmidt net) or equal angle (Wulff net). There is no set function in R available for this but contributed packages have already solved this problem.

For a Schmidt net we load the RFOC package and call a function,

```
JPOST(file="/Users/lees/Mss/SEIS_BOOK/Fmech/FIGS/nets.eps" , width=10, height=6)
library('RFOC')
par(mfrow=c(1,2))
net()
title(sub='Schmidt Equal Area Net')
Wnet()
title(sub='Wulff Equal Angle Net')
dev.off()
```

From here on out we will use the equal area stereonet, although all the following can be accomplished by Wulff nets. To plot a set of poles from the experiment, we invoke a few calls to built in functions,

```
az=c(-149,-154,-125,-142,-128,-123,-127,-137,-130,-130,-127,-150,
-138,-128,-141,-128,-143,-122,-130,-129,-158,-131,-128,-109,-134)
dip=c(54,62,52,53,53,45,43,50,54,52,54,53,54,53,56,52,54,46,54,48,51,
53,65,60,53)
```

In this case dip angles are apparently measured from the zenith, as one would for an upper hemispherical projection.

If we want to know the mean vector summarizing these points we cannot simply average the inclination and declination angles. This would lead to serious errors in many applications. Rather the poles should be converted to Cartesian coordinates, then averaged and, if necessary, the resultant

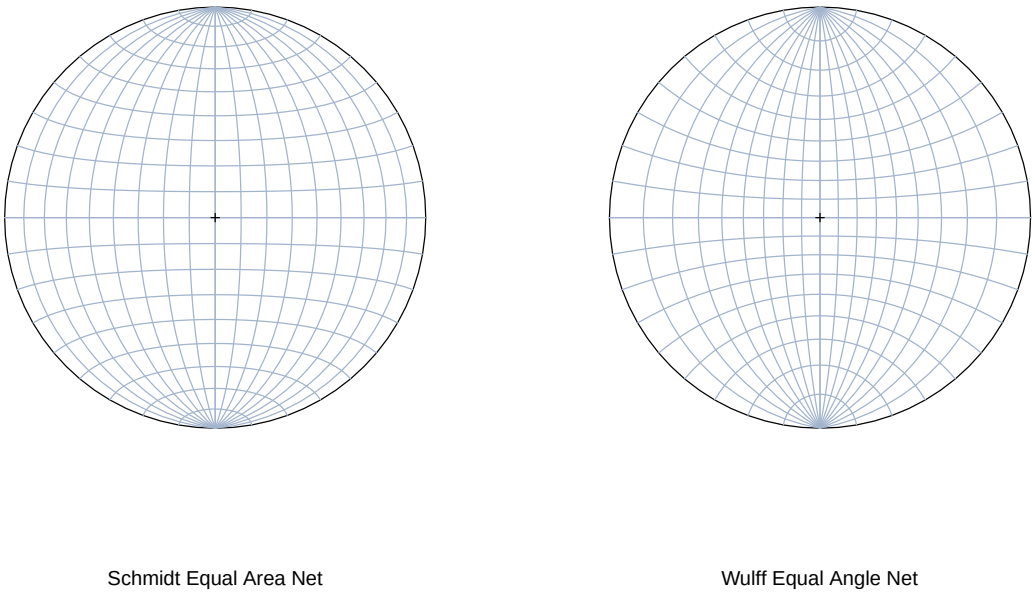

Figure 7: Schmidt (Equal Area) and Wulff (Equal Angle) Nets

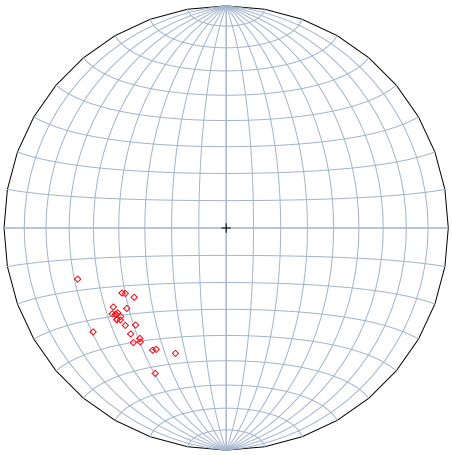

Figure 8: Schmidt Net with observations plotted

vector is converted back to polar form. The formulas derived above are applied to all the vectors, such that, if the angles are given in degrees, we can form a matrix of Cartesian vectors,

```
DEG2RAD = pi/180
   a = dip * DEG2RAD
   b = (az) * DEG2RAD
   x = sin(a) * cos(b)
   y = sin(a) * sin(b)
   z = cos(a)
   v = cbind(x, y, z)
```

The matrix v consists of three columns, representing the x,y,z coordinates of each pole. N is the number of poles in our data set. To get the summary vectors we average the N Cartesian coordinates individually, first by taking the sums

$$R_e = \sum x_i \tag{0.7}$$

$$R_n = \sum y_i \tag{0.8}$$

$$R_d = \sum z_i \tag{0.9}$$

The length of this vector is R,

$$R = \sqrt{R_e^2 + R_n^2 + R_d^2} \tag{0.10}$$

and, of course the average direction is $R_e/N, R_n/N, R_d/N$. If R is is close to 1 the vectors are dispersed randomly around the sphere. On the other hand if R is close to N the vectors are nearly all aligned in the same direction. The precision parameter (K) can be thus formed by taking the

$$K = \frac{(N-1)}{(N-R)} \tag{0.11}$$

The precision parameter provides an estimate of the standard deviation (in degrees) of the vector poles via the approximation,

$$S \approx \frac{81^\circ}{\sqrt{K}} \tag{0.12}$$

In R the sum of the coordinates is the mean vector, and the inverse coordinate transformation is applied to get the resultant pole.

```
Rn = sum(y)
    Re = sum(x)
    Rd = sum(z)
    N = length(x)
    Ir = 180 * atan2( sqrt(Rn^2 + Re^2), Rd)/pi
    Dr = 180 * atan2(Re, Rn)/pi
```

We can now plot the full data set with the resultant mean orientation (blue triangle),

```
JPOST(file="/Users/lees/Mss/SEIS_BOOK/Fmech/FIGS/netpoint2.eps" , width=16, height=10)
####  X11(w=16, h=10)
pnet(MN)
PTS = qpoint(az, dip, UP=FALSE,  col=2)
PTS = qpoint(Dr, Ir, UP=FALSE,  col='blue', pch =2, cex=1.5)
dev.off()
```

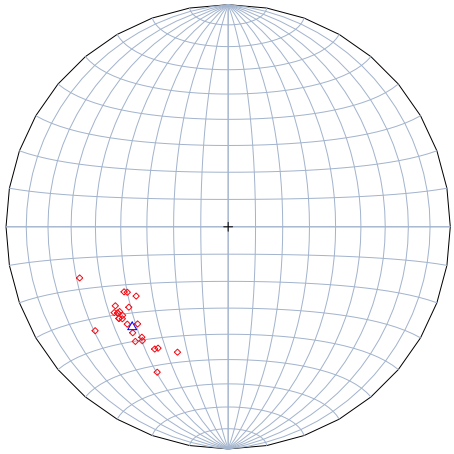

Figure 9: Schmidt Net, observations and mean vector plotted

The next step is to provide an estimate of the precision. This approximation is good if $R/n < 0.095$

```
R = sqrt(Rn^2 + Re^2 + Rd^2)
    K = (N - 1)/(N - R)
    S = 81/sqrt(K)
```

We can see that R is much greater than 1, close to N so the precision parameter K is large and there is high precision. The standard deviation in this case is about 10°.

Finally an estimate of the 95% confidence bounds may be estimated

$$\alpha_{95} = \arccos\left(1 - (N - R)\, 20^{\frac{1}{N-1}}\right) \tag{0.13}$$

```
alpha=1-0.95
Alpha95 = 180 * acos(1 - ((N - R) * (((1/alpha)^(1/(N - 1))) - 1)/R))/pi
JPOST(file="/Users/lees/Mss/SEIS_BOOK/Fmech/FIGS/netpoint3.eps" , width=16, height=10)
####  X11(w=16, h=10)
pnet(MN)
jj = qpoint(az, dip, UP=FALSE,  col=2)
jj =  qpoint(Dr, Ir, UP=FALSE,  col='black', pch=6)
jj = addsmallcirc(Dr, Ir, Alpha95, lty=1, lwd=2)
dev.off()
#####  acos(1+(log(0.05/(K*R))  ))/DEG2RAD
```

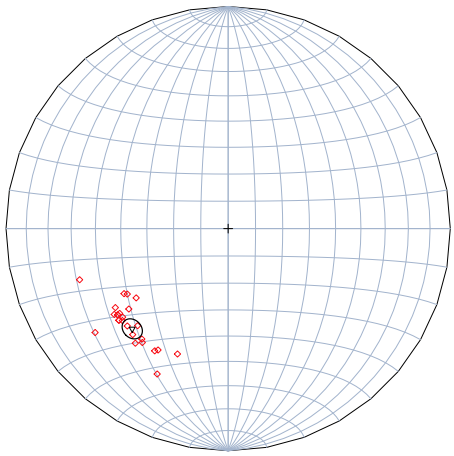

Figure 10: 95 % confidence bound for data

The last step is to provide a quantitative estimate of the clustering of the points. If the points are show a girded distribution versus a very pointed distribution this can be represented by replacing the distribution by an equivalent ellipse that captures the essence of the distribution on the sphere. If the ellipse is very elongate, the points are clustered tightly in a a narrow area. If they are randomly distributed, however, the ellipse will be nearly spherical. This can be summarized in a single coefficient κ which is derived from the eigenvalue decomposition of the variance-covariance

matrix of Cartesian vectors. The matrix is a measure of the distance each point is from a (special) axis, much like the moment of inertia of a body in physics. If the Cartesian coordinates are stored in an N by 3 matrix v, this is achieved by calculating,

$$B = \begin{bmatrix} N & 0 & 0 \\ 0 & N & 0 \\ 0 & 0 & N \end{bmatrix} - \begin{bmatrix} \sum x_i x_i & \sum x_i y_j & \sum x_i z_j \\ \sum y_i x_j & \sum y_i y_i & \sum y_i z_j \\ \sum z_i x_j & \sum z_i y_j & \sum z_i z_i \end{bmatrix} \tag{0.14}$$

Eigenvectors and eigenvalues can extracted for this matrix, although most authors simply calculate the Eigenvalues of the second matrix on the right hand side, the variance-covariance matrix Ψ. (We note that [Davis, 2002] does not mention this discrepancy. See [Woodcock, 1977]) The eigenvectors represent directions along which variance is maximized or minimized. In R these are obtained with the function $eigen()$. The cluster coefficient is the log eigenvalue ratios,

$$\kappa = \frac{\log\left(\frac{\epsilon_1}{\epsilon_2}\right)}{\log\left(\frac{\epsilon_2}{\epsilon_3}\right)} \tag{0.15}$$

```
KapT = t(v) %*% v
B = length(x) * diag(3) - KapT
E1 = eigen(B)
E = eigen(KapT)
Kappa = log(E$values[1]/E$values[2])/log(E$values[2]/E$values[3])
```

The value of κ =2.76 shows that the data is clustered near a central vector. We can see this by calculating $\kappa =$ for a variety of sample distributions (Figure 11). Depending on the value of κ

say spatially distributed, one can give a measure of the concentration distributed in space.

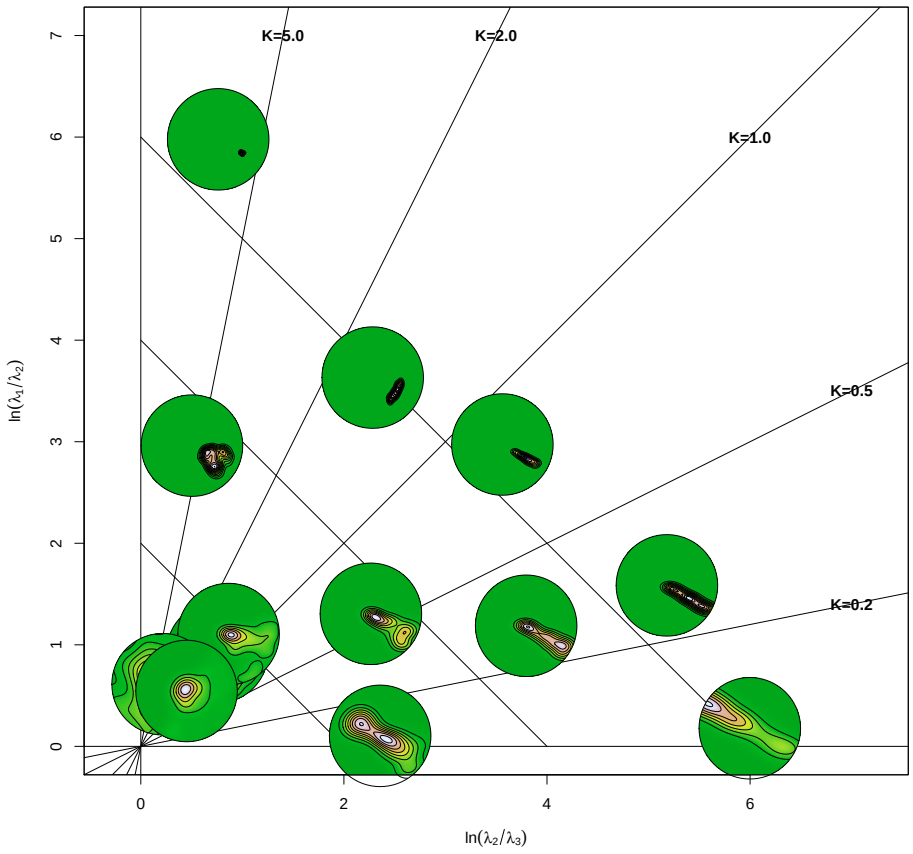

Figure 11: Kappa values and eigen value ratio classification

0.5 Example: Earthquake Focal Mechanisms

The application of stereonets can be particularly useful for earthquake data where thousands of P and T-axes (pressure and tension) are distributed in laterally and in depth. The focal mechanism is a way geologists plot tensor quantities in space.

When earthquakes occur below the surface they radiate energy along two sets of orthogonal directions forming two sets of force couples called a double couple. (Landslides can radiate single couple patterns and explosions have an isotropic component.) The double solutions can be derived from the first motions at seismographic stations distributed at the surface by projecting the ray-paths of the waves back to the hypocenter and plotting the directions of the first motions on a stereographic projection of the focal sphere. The resulting solution is a set of two planes, one representing the actual fault plane where the earth ruptured, the other is called the auxiliary plane that also radiates energy towards the surface. The data consists of points on the focal sphere indicating whether the motion was away or towards the earthquake hypocenter. These are plotted and a set of best fitting orthogonal planes are determined, usually by grid search methods. An example is shown in Figure 1 where the actual seismograms are displayed for illustration. A set of poles (points on the sphere) are derived that relate geophysical information about the nature of the earthquake orientation and slip vector and the compressional and tensional radiation axes. The slip vectors correspond possibly to striations one might observe on the fault surface as the earth scrapes the two planes during rupture.

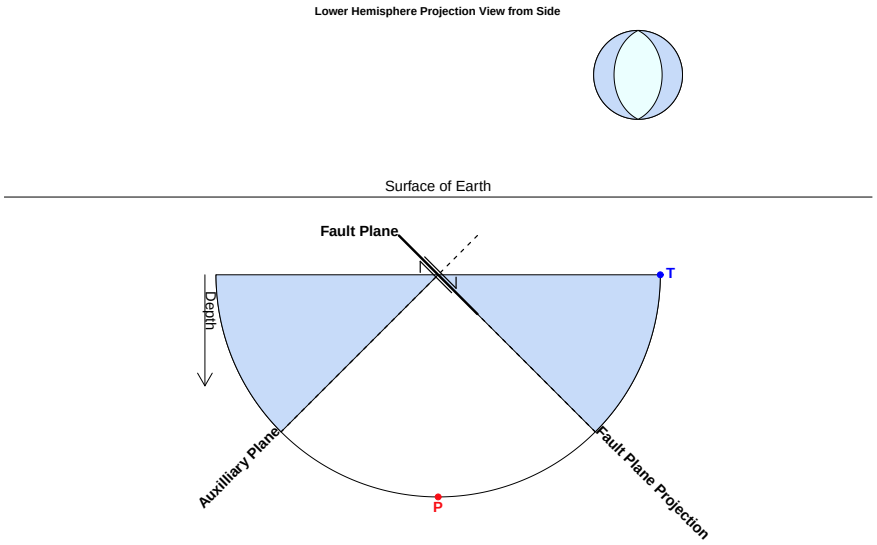

Figure 12: Earthquake Focal Mechanism

Strike slip, normal and reverse faults each have characteristic shapes and can represented in a visually revealing way be introducing the associated *beachball displays*.

An example of a typical representation of a focal mechanism for a fault strike-dip-rake of (65,

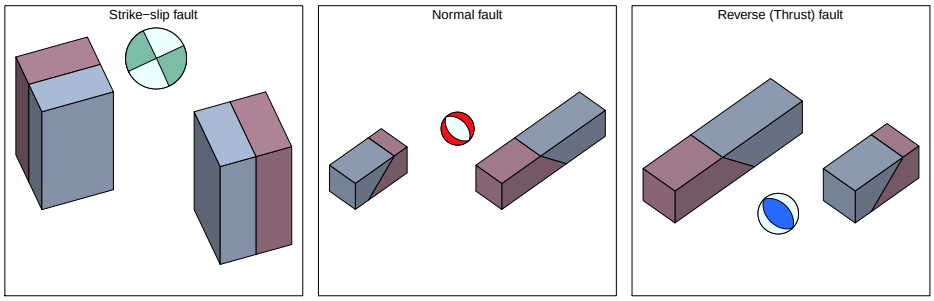

Figure 13: Examples of Faults and Focal Mechanisms

32, -34) is presented in Figure 14. Several of the relevant parameters are marked on this figure, although generally one only plots the colored hemispheres. The hemispheres show the investigator the orientation of the fault and auxiliary planes as seen from above projected on a lower hemisphere bowl. The colored region shows information about the radiation pattern of the seismic waves after rupture.

1 Map Views and Summary Representations

Once focal mechanisms are determined for each earthquake they can be plotted in map view using standard projections as a set of beach balls (Figure 15). The beach balls relate the nature of changing stress in the earth during earthquake swarms. In the Kamchatka example, there are thousands of beach-balls, some covering others which makes it difficult to discern important patterns.

In this case we can extract the P and T-axes from each focal mechanism and plot them all on one stereonet graph. Each P and T-axis is a vector in space derived from the focal mechanism. These are gathered together in one plot and statistical testing my be applied to determine if the distributions are uniform random, or clusters.

But really we are interested in the spatial distribution of P and T-axis across the Aleutian-Kamchatka Arc. To see how we might visualize this, we can break down the data (Figure 15) into small spatially distributed subsets. In each subset we project the P-T axes and contour or image the results, plotting them in their respective positions on the map. This provides a way to investigate variations in orientation of stress across a wide geologic region. As a further reduction of the data, one could calculate, plot and contour κ (concentration parameter) for each region to see how stress is focused in some regions and disbursed in others. I will leave that exercise to the reader.

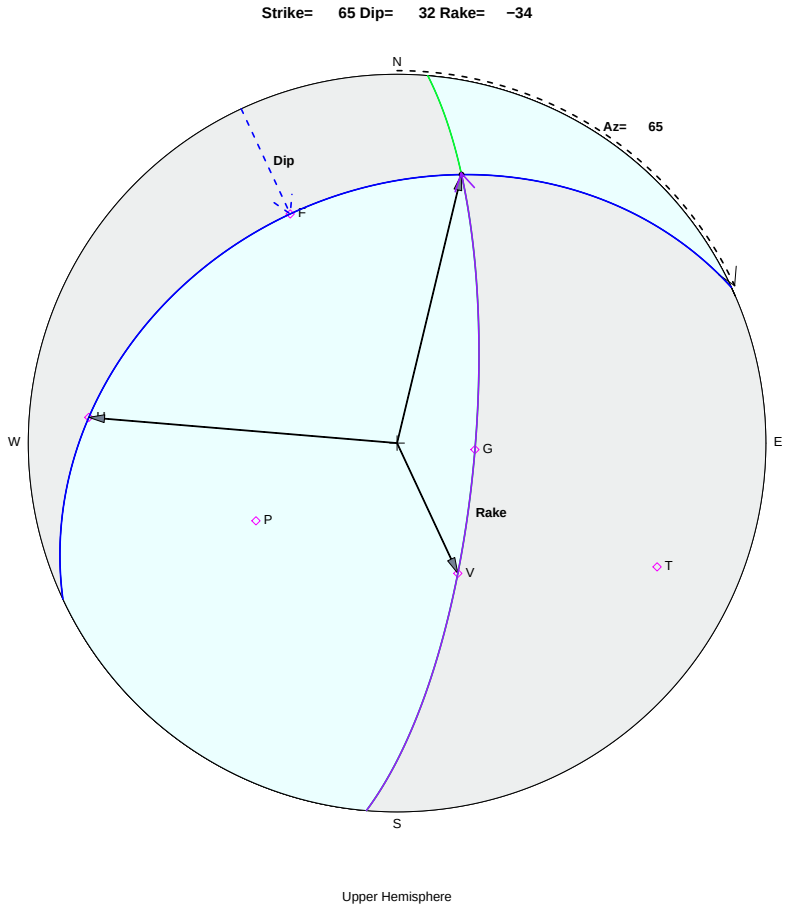

Figure 14: Earthquake Focal Mechanism

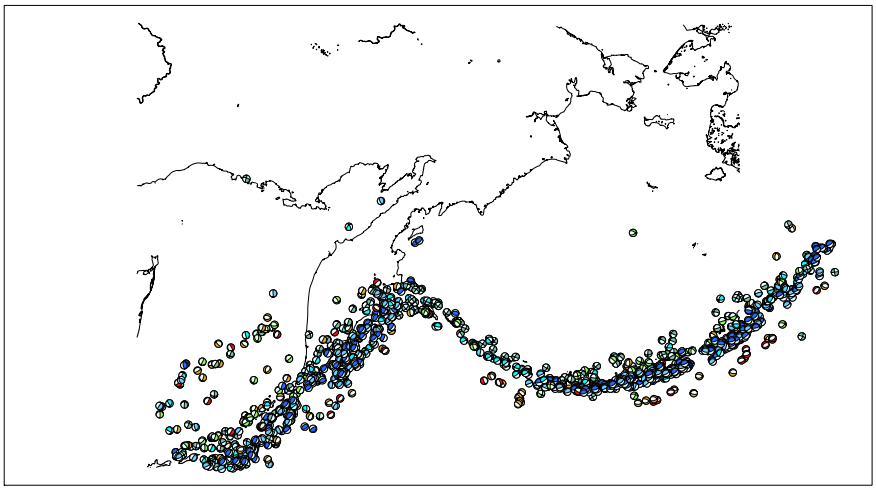

Figure 15: Kamchatka focal mechanisms

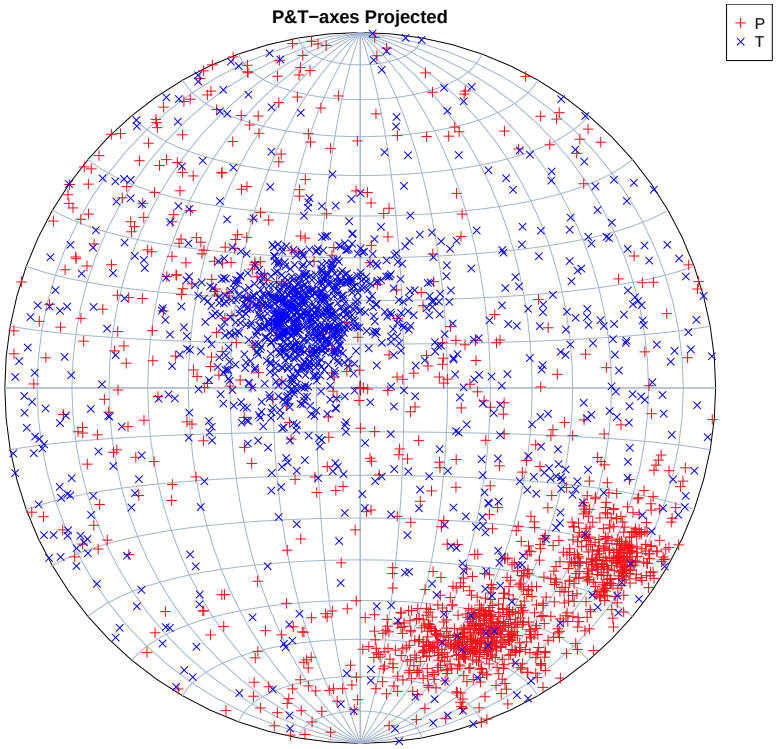

Figure 16: Kamchatka P-T axes

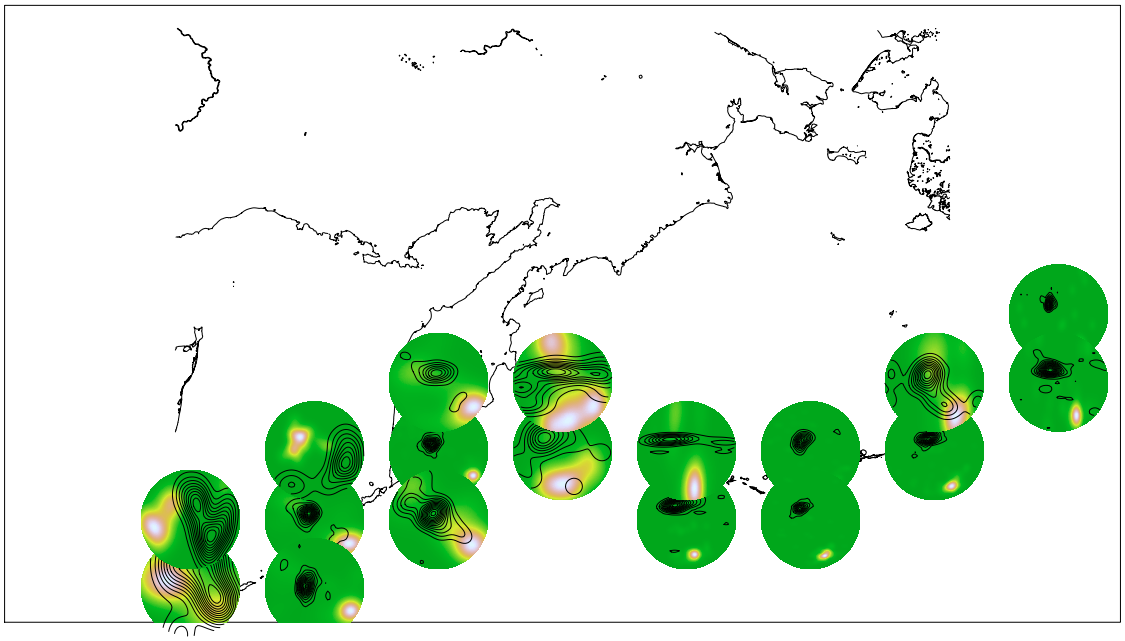

Figure 17: Geographic plot of Aleutian-Kamchatka P-T axes

References Cited

References

J. C. Davis. *Statistics and data analysis in geology*. Wiley, New York Chichester, 2002.

N. I. Fisher. *Statistical analysis of circular data*. Cambridge University Press, Cambridge [England] ; New York, NY, USA, 1993.

K. Mardia. *Statistics of Direction Data*. Academic press, New York, 1972.

T. L. N. I. Fisher and B. J. J. Emgleton. *Statistical analysis of spherical data*. Cambridge University Press, Cambridge [Cambridgeshire] ; New York, 1987.

N. H. Woodcock. Specification of fabric shapes using an eigenvalue method. *Geological Society of America Bulletin*, 88(9):1231–1236, 1977.